Hadron Spectra Parameters within the Non-Extensive Approach [†]

Keming Shen *[ID], **Gergely Gábor Barnaföldi** [‡][ID] **and Tamás Sándor Biró** [‡][ID]

Wigner Research Center for Physics of HAS, 29-33 Konkoly-Thege Miklós Street, 1121 Budapest, Hungary; barnafoldi.gergely@wigner.mta.hu (G.G.B.); biro.tamas@wigner.mta.hu (T.S.B.)
* Correspondence: shen.keming@wigner.mta.hu
† This paper is based on my talk at the 18th Zimányi School, Budapest, Hungary, 3–7 December 2018.
‡ These authors contributed equally to this work.

Abstract: We investigate how the non-extensive approach works in high-energy physics. Transverse momentum (p_T) spectra of several hadrons are fitted by various non-extensive momentum distributions and by the Boltzmann–Gibbs statistics. It is shown that some non-extensive distributions can be transferred one into another. We find explicit hadron mass and center-of-mass energy scaling both in the temperature and in the non-extensive parameter, q, in proton–proton and heavy-ion collisions. We find that the temperature depends linearly, but the Tsallis q follows a logarithmic dependence on the collision energy in proton–proton collisions. In the nucleus–nucleus collisions, on the other hand, T and q correlate linearly, as was predicted in our previous work.

Keywords: transverse momentum spectra; non-extensive; heavy-ion collisions

1. Introduction

In high-energy nuclear physics, the investigation of transverse momentum (p_T) spectra is a fundamental measure in statistical approaches. The p_T spectrum reveals information on the kinetic properties of the particles produced in high-energy collisions. Strong correlation phenomena were recently observed in proton–proton and heavy-ion collisions [1,2], their statistical and thermodynamical description points beyond the classical Boltzmann–Gibbs (BG) statistics. It has long been realized that data on single inclusive particle distributions show a power-law behavior in the high-p_T region. For these, the Pareto–Hagedorn–Tsallis distribution has been frequently applied [3–5]. Its form coincides with the generalized q-exponential function [6]:

$$\mathrm{e}_q(x) := [1 + (1-q)x]^{\frac{1}{1-q}} . \tag{1}$$

Hadron spectra can be described by the Lorentz-invariant particle spectra. These were successfully fitted by the non-extensive distributions in a wide center-of-mass energy and p_T range [7–20]. In the following, we focus on the most often used formulas from [7–15] for representing identified particle spectra in various collisions. This work explores differences between ($m_T - m$) and m_T-dependent, as well as simple p_T functions:

$$E \frac{\mathrm{d}^3 N}{\mathrm{d}^3 p} = \frac{\mathrm{d}^3 N}{\mathrm{d}y\, p_T\, \mathrm{d}p_T\, \mathrm{d}\phi} = \frac{1}{2\pi p_T} \frac{\mathrm{d}^2 N}{\mathrm{d}y\, \mathrm{d}p_T}. \tag{2}$$

Different research groups used various kinds of expressions of it in order to describe p_T spectra. We consider functions of $m_T - m$ and p_T in the non-extensive approach, after applying the normalized

functions and the thermodynamically motivated ones [21]. Our aim is to find the best-fitting functions among these, while assigning a physical interpretation to their parameters. We investigate the following distribution forms:

$$f_0 = f_{BG} = A_0 \cdot \exp\left(\frac{m_T - m}{T_0}\right),$$

$$f_1 = A_1 \cdot \left(1 + \frac{m_T - m}{n_1 T_1}\right)^{-n_1},$$

$$f_2 = A_2 \cdot \frac{(n_2 - 1)(n_2 - 2)}{2\pi n_2 T_2 [n_2 T_2 + m(n_2 - 2)]} \cdot \left(1 + \frac{m_T - m}{n_2 T_2}\right)^{-n_2},$$

$$f_3 = A_3 \cdot m_T \left(1 + \frac{m_T - m}{n_3 T_3}\right)^{-n_3},$$

$$f_4 = A_4 \cdot \left(1 + \frac{m_T}{n_4 T_4}\right)^{-n_4},$$

$$f_5 = A_5 \cdot \left(1 + \frac{p_T}{n_5 T_5}\right)^{-n_5}. \tag{3}$$

There are relations among the distributions defined above. It is easy to realize that f_1 and f_2 coincide whenever their amplitudes satisfy the relation

$$A_1 = A_2 \cdot \frac{(n_2 - 1)(n_2 - 2)}{2\pi n_2 T_2 [n_2 T_2 + m(n_2 - 2)]} = A_2 \cdot C_q, \quad \text{and} \quad n_1 = n_2. \tag{4}$$

Accounting for the differences between $(m_T - m)$ and m_T dependencies, we re-cast f_1 and f_4 described in Equation (3) as follows:

$$f_1 = A_1 \cdot \left(1 - \frac{m}{n_1 T_1}\right)^{-n_1} \cdot \left(1 + \frac{m_T}{n_1 T_1 - m}\right)^{-n_1}. \tag{5}$$

Comparing this with f_4, we arrive at the relations

$$A_1 \cdot \left(1 - \frac{m}{n_1 T_1}\right)^{-n_1} = A_4, \quad n_1 = n_4, \quad \text{and} \quad n_1 T_1 - m = n_4 T_4. \tag{6}$$

These comments are important for the comparison of different approaches. They also demonstrate that no inconsistency occurs by applying different fit formulas. However, differences arise from the statistical physical motivations behind these formulas [7–12,21,22]. The corresponding results and discussions are investigated next. Note that for all the physical quantities, we use the natural units, $c = 1$, for convenience in this paper.

2. Results and Discussions

In this section, we analyze the transverse momentum distributions of identified pions and kaons stemming from the elementary (pp) and heavy-ion (pPb and $PbPb$) collisions fitted by the functions listed in Equation (3). All the relevant parameters are then analyzed in order to investigate further the non-extensive physics behind these collisions.

2.1. Analysis of the pp Spectra

In high-energy physics, even the smallest hadron–hadron (pp) collisions are rather complicated processes. One usually separates two main regimes of hadron production: one is a soft multiparticle production, dominant at low transverse momenta, where the spectra can also be fitted by an exponential behavior [23], cf. the curve f_{BG} in Figure 1. We realize that f_{BG} describes well this part of the spectra even in pp collisions. As p_T gets higher ($p_T > 3$ GeV), the spectrum displays a power-law tail. They are

predicted by perturbative QCD, owing to the hard scattering of current quarks and gluons. In a number of publications [16–20], the Tsallis statistical distribution was successfully applied to describe data for *pp* collisions over a wide range of the transverse momenta because of its two limits: the exponential shape at small p_T and the power-like distribution at large p_T,

$$e_q(-\frac{p_T}{T}) \longrightarrow \begin{cases} e^{-p_T/T} & p_T \to 0 \\ \\ \left((q-1)\frac{p_T}{T}\right)^{\frac{1}{1-q}} & p_T \to \infty. \end{cases} \tag{7}$$
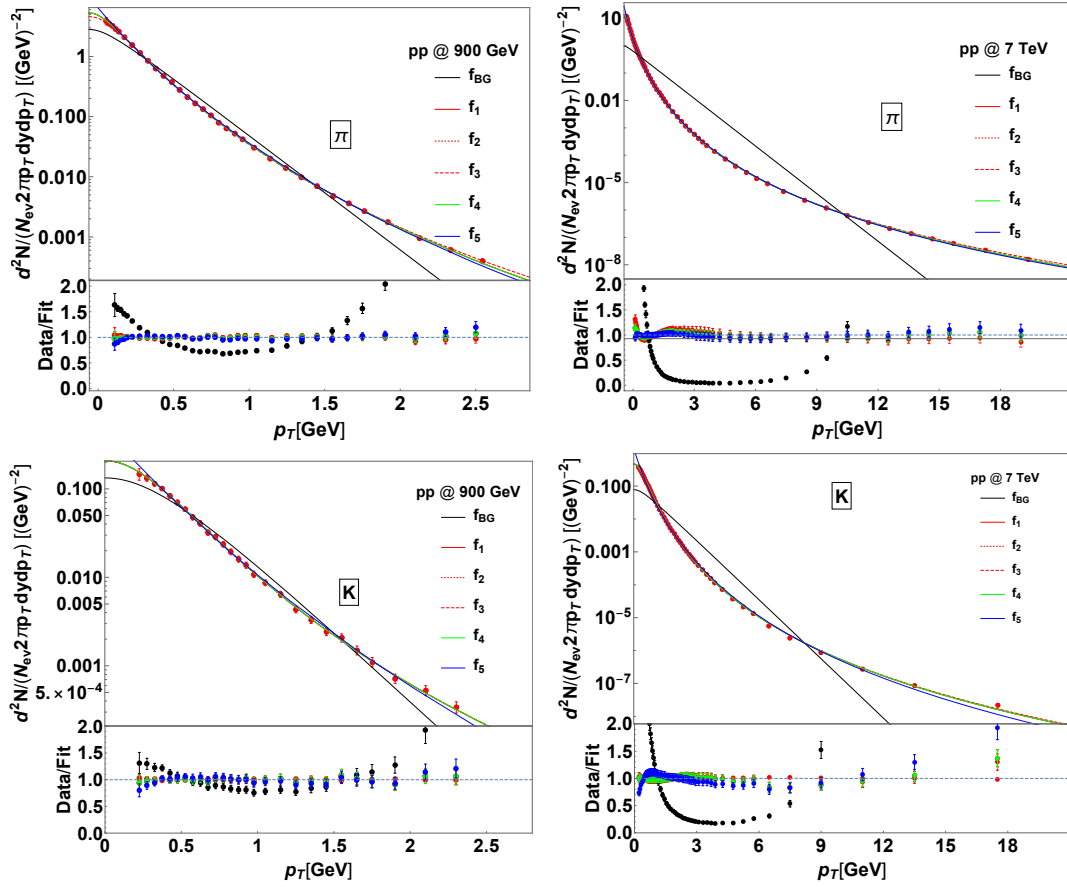

Figure 1. The p_T spectra for pions (upper) and kaons (lower) in *pp* collisions at $\sqrt{s} = 900$ GeV and 7 TeV at midrapidity as examples. Data are taken from [16,17]. All are fitted with all of the functions of Equation (3) in the ranges of $0.1 < p_T < 2.6$ GeV at $\sqrt{s} = 900$ GeV and $0.1 < p_T < 20$ GeV at 7 TeV, respectively. Ratios of the net fits to data are also shown in the lower panel. The relevant values of $\chi^2/d.o.f.$ are shown in Table 1.

Table 1. The values of $\chi^2/d.o.f.$ of spectral fits for pions, kaons, and protons in *pp* collisions at 900 GeV and 7 TeV as examples.

Collision Energy ($\sqrt{s}$)	Produced Hadrons	f_{BG}	f_1	f_2	f_3	f_4	f_5
	π	110.8	0.2814	0.2814	0.4697	0.2814	1.456
900 GeV	K	8.047	0.1748	0.1749	0.1698	0.1749	0.6669
	p	3.491	0.3724	0.3724	0.3735	0.3724	0.4145
	π	1316.0	0.9681	0.9681	3.417	0.9681	0.3049
7 TeV	K	520.2	0.4202	0.4202	0.4313	0.4202	3.100
	p	254.3	0.4481	0.4481	0.4356	0.4481	4.357

We focus on the fittings of the produced charged particle spectra in elementary collisions with the non-extensive functions in Equation (3). Data were taken for pions, kaons, and protons in pp collisions at $\sqrt{s} = 62.4$ GeV, 200 GeV from the PHENIX Collaboration [18] and at 900 GeV [16], 2.76 TeV [19], 5.02 TeV, and 7 TeV [17] from the ALICE Collaboration. We restrict our analysis to the midrapidity region $|y| < 0.5$ within the p_T ranges, as shown in Table 2. Note that in the following, π, K, and p mark the spectra of $\frac{\pi^+ + \pi^-}{2}$, $\frac{K^+ + K^-}{2}$, and $\frac{p + \bar{p}}{2}$, respectively.

Table 2. Fitting p_T ranges of spectra for different charged particles in pp collisions [16–19].

$\sqrt{s}$	π [GeV]	K [GeV]	p [GeV]
62.4 GeV	0.3–2.9	0.4–2	0.6–3.6
200 GeV	0.3–3	0.4–2	0.5–4.6
900 GeV	0.1–2.6	0.2–2.4	0.35–2.4
2.76 TeV	0.1–20	0.2–20	0.3–20
5.02 TeV	0.1–20	0.2–20	0.3–20
7 TeV	0.1–20	0.2–20	0.3–20

Figure 1 shows that all of the different non-extensive functions we used fit the pion and kaon spectra very well for various kinds of beam energies at midrapidity. The ratios of $\chi^2/d.o.f.$ of the relevant fits are given in Table 1. Specifically, the first two distributions (f_1 and f_2) of $m_T - m$ and f_4 of m_T show close-fitting results. The distribution, f_3, derived thermodynamically, does not display large differences in the goodness of fit either. Checking the fitting parameters A, T, and $q = 1 + 1/n$, we observe that, as we expected and introduced in the previous section, all these functions share the same Tsallis parameter n. The two $m_T - m$ functions (f_1 and f_2) lead to fitting values of the temperature T, which are different from the pure m_T fit (f_4). This indicates that the normalization constant does not affect the fitted T and q parameters but the integrated yield dN/dy. Namely, by normalizing the momentum spectrum

$$\frac{1}{2\pi p_T} \frac{d^2 N}{dy\, dp_T} = A_2 \cdot C_q \cdot \left(1 + \frac{m_T - m}{n_2 T_2}\right)^{-n_2} \tag{8}$$

with the C_q normalization constant and the condition of $A_2 = dN/dy$, we obtain the integral over p_T from 0 to its maximal values p_{Tmax}:

$$\int_0^{p_{Tmax}} \frac{1}{2\pi p_T} \frac{d^2 N}{dy\, dp_T} 2\pi p_T\, dp_T = \frac{dN}{dy} . \tag{9}$$

Moving towards physical interpretation issues, we investigate the temperature, T, and the non-extensive parameter, q. Investigations in [18,24] showed that both of them express $\sqrt{s}$ dependence. In this paper, we found that they are also dependent on the hadron mass, m. The $\sqrt{s}/m$ dependence, as a result, is studied in order to analyze hadron spectra parameters within the non-extensive approach. Following the phenomenological observations in [25,26], a QCD-like evolution can be introduced for both the parameters T and q. While analyzing data, we found that the temperature T had a weak logarithmic $\sqrt{s}/m$ dependence. Thus, here we assume a linear $\sqrt{s}/m$ dependence to analyze the temperature T, but the non-extensive parameter q is kept with the stronger logarithmic distribution:

$$T = T_0 + T_1 \cdot \left(\frac{\sqrt{s}}{m}\right), \quad \text{and} \quad q = q_0 + q_1 \cdot \ln\left(\frac{\sqrt{s}}{m}\right). \tag{10}$$

In summary, our work indicates that the BG distribution is not suitable for describing the hadron spectra over a wide range of p_T. Comparisons of their corresponding fitting errors $\chi^2/d.o.f.$ show that both $m_T - m$ and m_T functions share the same goodness between f_1 and f_2, cf. Equation (3). Together with the thermodynamically derived f_3, all the non-extensive approaches ($f_1 \sim f_4$) follow the

experimental data accurately. The fitting temperature, T, is nearly constant when changing the ratio of the collision energy to hadron mass, $\sqrt{s}/m$. Specifically, distributions of f_1, f_2, f_4, and f_5 are described best with such a connection, as shown in the left panel of Figure 2. From Table 3, we also see that the slope parameters in these four cases are almost zero, which means that they are constant around some values. The non-extensive parameter q, on the other hand, follows a logarithmic dependence, agreeing with a pQCD-based motivation, cf. [21]. Note that our results on T and q are different from the work by Cleymans et al. [24]. Those authors parameterized this relation as a power-law.
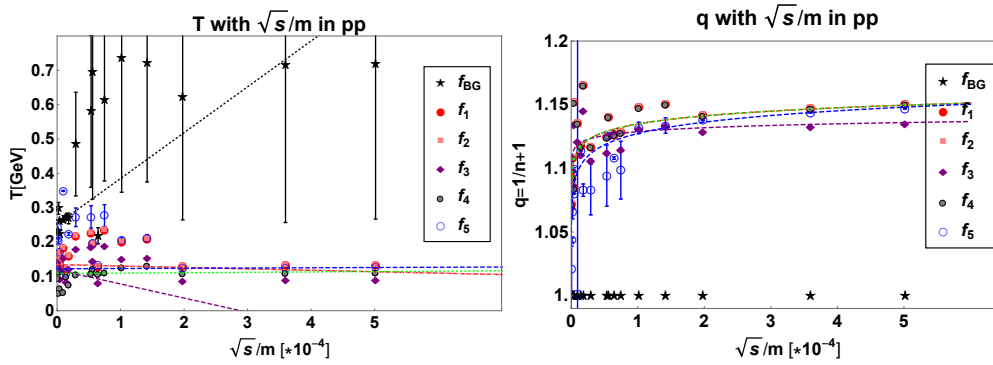

Figure 2. Both the center-of-mass energy $\sqrt{s}$ and hadron mass m distributions of the fitting temperature T and the non-extensive parameter q. In this work, we analyze the results at all given energies with the relationship cf. Equation (10). Here we list the results for $\sqrt{s}$ =62.4 GeV, 200 GeV, 900 GeV, 2.76 TeV, 5.02 TeV, and 7 TeV. and hadron species of pions, kaons, and protons. We have extracted a factor of 10^4 from the values of $\sqrt{s}/m$ for convenience.

Table 3. Fitting parameters of Equation (10) in use within Figure 2.

Fitting Functions	T_0	T_1	q_0	q_1
f_{BG}	0.2515 ± 0.0005	0.1335 ± 0.0002	-	-
f_1	0.1343 ± 0.0003	-0.0041 ± 0.0001	1.135 ± 0.002	0.009 ± 0.001
f_2	0.1343 ± 0.0003	-0.0041 ± 0.0001	1.135 ± 0.002	0.009 ± 0.001
f_3	0.1190 ± 0.0002	-0.0412 ± 0.0002	1.129 ± 0.001	0.004 ± 0.001
f_4	0.1083 ± 0.0003	0.0011 ± 0.0004	1.135 ± 0.002	0.009 ± 0.001
f_5	0.1222 ± 0.0005	0.0007 ± 0.0001	1.127 ± 0.002	0.013 ± 0.002

2.2. Analysis of the pPb and PbPb Results

In *pPb* [17] collisions at 5.02 TeV and in *PbPb* [27–30] collisions at 2.76 TeV, more kinds of hadron spectra are analyzed within the formulas of Equation (3). Data are taken from the ALICE Collaboration within wide p_T ranges, as seen in Table 4. We observe that all of them present good fittings over the whole range of p_T for each hadron at various kinds of centrality bins. On the other hand, similar to the *pp* cases, the BG formula can still perform well just in the low p_T region ($p_T < 3$ GeV).

Table 4. Fitting p_T range of different hadron spectra in heavy-ion collisions in this work [17,27–30].

Particles	Mass [GeV]	*pPb* [GeV]	*PbPb* [GeV]
π	0.140	0.11–2.85	0.11–19
K	0.494	0.225–2.45	0.225–19
K_S^0	0.498	0.05–7	0.45–11
K^*	0.896		0.55–4.5
p	0.938	0.325–3.9	0.325–17.5
ϕ	1.019		0.65–4.5
Λ	1.116	0.65–7	0.65–11
Ξ	1.321		0.7–7.5
Ω	1.672		1.3–7.5

In this work, as an example, we analyzed the fitting results of p_T spectra of pions and kaons produced in all kinds of collisions mentioned above. It is instructive to plot the relationship between the fitting temperature T and the Tsallis parameter q for the same hadron spectra for different centralities in the same heavy-ion collisions. The results of pions and kaons in pp collisions are also analyzed as comparisons. In Figure 3, we show the linear correlating appearances for both π and K in pPb at 2.76 TeV [17] and in $PbPb$ at 5.02 TeV [27,28] as well as the pp results in all kinds of collision energies [16–19] in this paper. In fact, whatever kinds of particle we study, all these non-extensive fittings give a similar dependence of T on the parameter q:

$$T \approx T_0 - (q-1)T_1 \,, \tag{11}$$

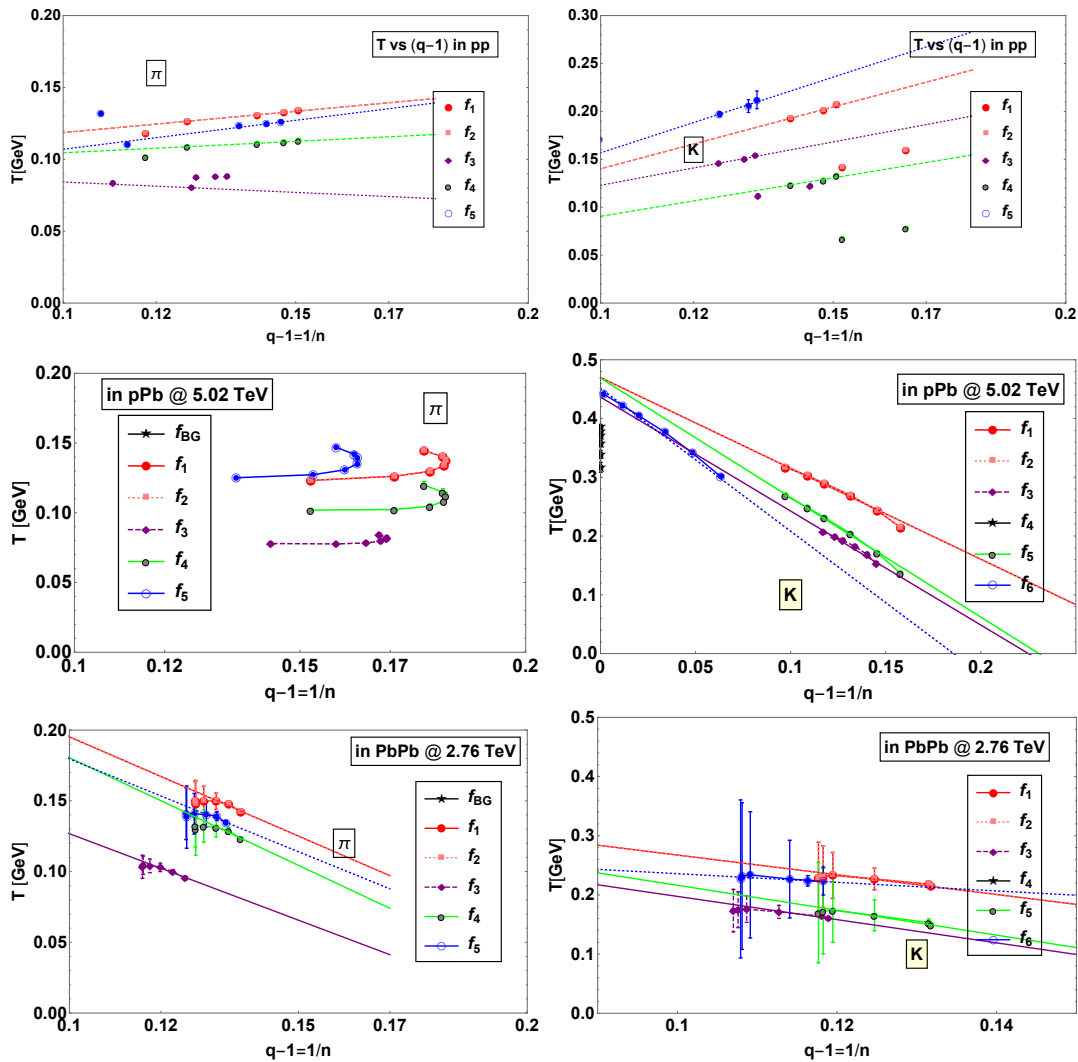which agrees with our previous work [21,22] and that of others [31].

Figure 3. Correlations between T and $q - 1 = 1/n$ for spectra of π (left) and K (right) in pp, pPb, and $PbPb$ collisions. The corresponding p_T range is listed in Table 4, and the values of fitting parameters in Equation (11) are listed in Table 5.

Note that the slope parameter T_1 in Table 5 turns negative and T_0 is nearly zero for the pp case, as discussed in [22]. Results of fittings on pion spectra, typically in pPb collisions at 5.02 TeV, fail in the obvious linear combinations probably due to the small mass of pions and high multiplicities. It is found that all forms of non-extensive distributions feature a similar relation between the temperature

T and non-extensive parameter q. This, in turn, hopefully promotes a better understanding of the meaning of the non-extensive parameter q.

Table 5. Fitting parameters of Equation (11) between T and $q - 1 = 1/n$ for spectra of π (upper) and K (lower) in pp, pPb, and $PbPb$ collisions (note that f_{BG} is not included because $q = 1$ is a constant).

Particles	Fittings	T_1 in pp	T_0 in pp	T_1 in pPb	T_0 in pPb	T_1 in $PbPb$	T_0 in $PbPb$
	f_1	-0.36 ± 0.02	0.08 ± 0.01	-	-	1.40 ± 0.02	0.335 ± 0.004
	f_2	-0.36 ± 0.02	0.08 ± 0.01	-	-	1.40 ± 0.02	0.335 ± 0.004
π	f_3	-0.14 ± 0.04	0.07 ± 0.02	-	-	1.22 ± 0.02	0.249 ± 0.005
	f_4	-0.22 ± 0.01	0.08 ± 0.01	-	-	1.52 ± 0.02	0.333 ± 0.005
	f_5	-0.31 ± 0.03	0.08 ± 0.01	-	-	1.31 ± 0.01	0.311 ± 0.007
	f_1	-1.30 ± 0.02	0.011 ± 0.001	1.55 ± 0.02	0.470 ± 0.001	1.67 ± 0.06	0.434 ± 0.003
	f_2	-1.30 ± 0.02	0.011 ± 0.001	1.55 ± 0.02	0.470 ± 0.001	1.67 ± 0.06	0.434 ± 0.003
K	f_3	-0.90 ± 0.04	0.032 ± 0.005	1.94 ± 0.03	0.436 ± 0.004	1.96 ± 0.03	0.394 ± 0.007
	f_4	-0.81 ± 0.01	0.010 ± 0.004	2.03 ± 0.03	0.470 ± 0.003	2.11 ± 0.05	0.427 ± 0.006
	f_5	-1.59 ± 0.02	-0.001 ± 0.0005	2.43 ± 0.01	0.453 ± 0.002	0.73 ± 0.02	0.309 ± 0.007

3. Summary

In this work, we analyzed various fitting formulas of the hadron spectra in order to explore their sensitivity to different fitting parameters in use within the non-extensive approaches, cf. Equation (3). The hadronization, as well as the p_T distributions in high-energy physics (in proton–proton, proton–nucleus, and nucleus–nucleus collisions) are being studied here. For more details, see [21].

Our results reveal that normalization parameters have no major effect on the shape of these functions. In other words, the fitting formulas of either $m_T - m$ or m_T lead to the same fit quality. As shown in Table 1, they obtained similar fitting values of $\chi^2/d.o.f.$. Finally, we investigated the relationship between the fitting parameters, T and q. In pp collisions, the temperature values were fitted by the linear relation of $\sqrt{s}/m$, while the non-extensive parameter q had a logarithmic $\sqrt{s}/m$ dependence, motivated by the QCD-like evolution [25,26]. All kinds of approaches led to linear relations between the temperature, T, and the non-extensive parameter, $q - 1$, in heavy-ion collisions at different centralities. This agrees well with our previous results [21,22] and others in [31].

Summarizing, based on the Tsallis q-exponential, five types of non-extensive formulas in Equation (3) were investigated in parallel to the usual BG distribution. Results showed that the BG statistics failed in describing the hadronization in the whole p_T range. Within the non-extensive approaches, $m_T - m$ functions obtained similar fitting results to the m_T ones. This provides a free choice between the functions $m_T - m$ and m_T when analyzing the hadron spectra. On the other hand, it does not make any differences with regards to the normalization. Nevertheless, the normalized function, f_2, is the best choice since it is also connected to the particle yield per unit rapidity, dN/dy, by its normalization, A_2.

Author Contributions: Authors contributed equally to the contribution.

Conflicts of Interest: The authors declare no conflict of interest. The funders had no role in the design of the study; in the collection, analyses, or interpretation of data; in the writing of the manuscript, or in the decision to publish the results.

Abbreviations

The following abbreviations are used in this manuscript:

p_T transverse momentum
BG   Boltzmann–Gibbs
m_T transverse mass

References

1. ALICE Collaboration. Enhanced production of multi-strange hadrons in high-multiplicity proton-proton collisions. *Nat. Phys.* **2017**, *13*, 535–539.
2. ALICE Collaboration. ALICE measures pA collisions: Collectivity in small systems? *J. Phys. Conf. Ser.* **2017**, *798*, 012068.
3. Pareto, V. *Cours d'Economie Politique*; Droz: Geneva, Switzerland, 1896.
4. Hagedorn, R.; Multiplicities, T. p_T distributions and the expected hadron $\rightarrow$ quark-gluon phase transition. *Riv. Nuovo Cimento* **1983**, *6*, 1–50. [CrossRef]
5. Tsallis, C. Possible generalization of Boltzmann-Gibbs statistics. *J. Stat. Phys.* **1988**, *52*, 479–487. [CrossRef]
6. Tsallis, C. Generalizing What We Learnt: Nonextensive Statistical Mechanics. In *Introduction to Nonextensive Statistical Mechanics*; Springer: New York, NY, USA, 2009; p. 382.
7. Osada, T.; Wilk, G. Nonextensive hydrodynamics for relativistic heavy-ion collisions. *Phys. Rev. C* **2008**, *77*, 044903. [CrossRef]
8. STAR Collaboration. Identified Baryon and Meson Distributions at Large Transverse Momenta from $Au + Au$ Collisions at $\sqrt{s_{NN}} = 200$ GeV. *Phys. Rev. Lett.* **2006**, *97*, 152301.
9. BRAHMS Collaboration. Charged Meson Rapidity Distributions in Central $Au + Au$ Collisions at $\sqrt{s_{NN}} = 200$ GeV. *Phys. Rev. Lett.* **2005**, *94*, 162301.
10. CMS Collaboration. Transverse momentum and pseudorapidity distributions of charged hadrons in pp collisions at sqrt(s) = 0.9 and 2.36 TeV. *J. High Energy Phys.* **2010**, *2010*, 41.
11. CMS Collaboration. Transverse-Momentum and Pseudorapidity Distributions of Charged Hadrons in pp Collisions at $\sqrt{s} = 7$ TeV. *Phys. Rev. Lett.* **2010**, *105*, 022002.
12. PHENIX Collaboration. Identified charged particle spectra and yields in $Au + Au$ collisions at $\sqrt{s_{NN}} = 200$ GeV. *Phys. Rev. C* **2004**, *69*, 034909.
13. STAR Collaboration. Identified hadron spectra at large transverse momentum in $p + p$ and $d + Au$ collisions at $\sqrt{s_{NN}} = 200$ GeV. *Phys. Lett. B* **2006**, *637*, 161–169.
14. STAR Collaboration. $K(892)^*$ Resonance Production in $Au + Au$ and $p + p$ Collisions at $\sqrt{s_{NN}} = 200$ GeV at RHIC. *Phys. Rev. C* **2005**, *71*, 064902.
15. Wilk, G.; Wlodarczyk, Z. Interpretation of the Nonextensivity Parameter q in Some Applications of Tsallis Statistics and Lévy Distributions. *Phys. Rev. Lett.* **2000**, *84*, 2770–2773. [CrossRef] [PubMed]
16. ALICE Collaboration. Production of pions, kaons and protons in pp collisions at $\sqrt{s} = 900$ GeV with ALICE at the LHC. *Eur. Phys. J. C* **2011**, *71*, 1655.
17. ALICE Collaboration. Multiplicity Dependence of Pion, Kaon, Proton and Lambda Production in $p + Pb$ Collisions at $\sqrt{s_{NN}} = 5.02$ TeV. *Phys. Lett. B* **2014**, *728*, 25–38.
18. PHENIX Collaboration. Identified charged hadron production in $p + p$ collisions at $\sqrt{s} = 200$ and 62.4 GeV. *Phys. Rev. C* **2011**, *83*, 064903.
19. ALICE Collaboration. Production of charged pions, kaons and protons at large transverse momentum in pp and $Pb - Pb$ collisions at $\sqrt{s_{NN}} = 2.76$ TeV. *Phys. Lett. B* **2014**, *736*, 196–207.
20. Tang, Z.; Xu, Y.; Ruan, L.; van Buren, G.; Wang, F.; Xu, Z. Spectra and radial flow in relativistic heavy ion collisions with Tsallis statistics in a blast-wave description. *Phys. Rev. C* **2009**, *79*, 051901. [CrossRef]
21. Shen, K.; Barnaföldi, G.G.; Biró, T.S. Hadronization within Non-Extensive Approach and the Evolution of the Parameters. *arXiv* **2019**, arXiv:1905.05736.
22. Shen, K.M.; Biro, T.S.; Wang, E.K. Different non-extensive models for heavy-ion collisions. *Phys. A* **2018**, *492*, 2353–2360. [CrossRef]
23. Hagedorn, R. *Hot and Hadronic Matter: Theory and Experiment*; Plenum Press, Publishing House: New York, NY, USA, 1995; p. 13.
24. Cleymans, J.; Lykasov, G.I.; Parvan, A.S.; Sorin, A.S.; Teryaev, O.V.; Worku, D. Systematic properties of the Tsallis distribution: Energy dependence of parameters in high energy p-p collisions. *Phys. Lett. B* **2013**, *723*, 351–354. [CrossRef]
25. Barnaföldi, G.G.; Ürmössy, K.; Biró, T.S. Tsallis–Pareto–like Distributions in Hadron-Hadron Collisions. *J. Phys. Conf. Ser.* **2011**, 270, 357–363. [CrossRef]
26. Takacs, A.; Barnaföldi, G.G. Non-Extensive Motivated Parton Fragmentation Functions. *Multidiscipl. Digit. Publ. Inst. Proc.* **2019**, *10*, 12. [CrossRef]

27. ALICE Collaboration. Centrality dependence of the nuclear modification factor of charged pions, kaons, and protons in $Pb - Pb$ collisions at $\sqrt{s_{NN}}$ = 2.76 TeV. *Phys. Rev. C* **2016**, *93*, 034913.

28. ALICE Collaboration. K_S^0 and Λ Production in $Pb - Pb$ Collisions at $\sqrt{s_{NN}}$ = 2.76 TeV. *Phys. Rev. Lett.* **2013**, *111*, 222301.

29. ALICE Collaboration. Multi-strange baryon production at mid-rapidity in $Pb - Pb$ collisions at $\sqrt{s_{NN}}$ = 2.76 TeV. *Phys. Lett. B* **2014**, *728*, 216.

30. ALICE Collaboration. $K^*(892)^0$ and $\phi(1020)$ production in $Pb - Pb$ collisions at $\sqrt{s_{NN}}$ = 2.76 TeV. *Phys. Rev. C* **2015**, *91*, 024609.

31. Wilk, G.; Włodarczyk, Z. On possible origins of power-law distributions. *AIP Conf. Proc.* **2015**, *1558*, 893–896, and its corresponding references.